

## Coexisting retrograde jadeite and omphacite in a jadeite-bearing lawsonite eclogite from the Motagua Fault Zone, Guatemala

TATSUKI TSUJIMORI,\* JUHN G. LIOU, AND ROBERT G. COLEMAN

Department of Geological and Environmental Sciences, Stanford University, Stanford, California 94305, U.S.A.

### ABSTRACT

Coexisting jadeite and omphacite were found as retrograde minerals in a jadeite-bearing lawsonite-eclogite from the Motagua Fault Zone, Guatemala. The lawsonite-eclogite is characterized by the occurrence of garnet porphyroblasts up to 2.5 cm in size, and the eclogite-facies parageneses, almandine-rich garnet + impure jadeite + lawsonite + rutile + quartz; garnet contains inclusions of impure jadeite, phengite, ferroglaucophane, chlorite, lawsonite, rutile, ilmenite, and quartz. Textural relations and parageneses and compositions of minerals indicate that the lawsonite-eclogite experienced two stages of metamorphism: prograde eclogite-facies stage ( $M_1$ ) and retrograde stage ( $M_2$ ). The impure jadeite (Jd-I) of the  $M_1$  eclogite-facies occurs in both the matrix and as inclusions in garnet, and contains considerable amounts of augite and aegirine components ( $Jd_{61.75}Aug_{16.24}Ae_{0.18}$ ). It is partly recrystallized to retrograde  $M_2$  jadeite (Jd-II) ( $Jd_{74.87}Aug_{9.16}Ae_{0.11}$ ) and omphacite ( $Jd_{42.50}Aug_{36.46}Ae_{7.16}$ ); some of these two sodic pyroxenes may have crystallized from fluids. Both  $M_2$  jadeite and omphacite show textural equilibrium and are believed to have grown concurrently. Based on the observed compositions and the phase relations of sodic pyroxenes from Carpenter (1980), the  $M_1$  impure jadeite (Jd-I) may have had a disordered  $C2/c$  symmetry at  $T = ca. 450\text{ }^\circ\text{C}$  and  $P = ca. 1.8\text{--}2.4\text{ GPa}$ , and was subsequently crystallized into jadeite (Jd-II) plus ordered  $P2/n$  omphacite during retrogression with infiltration of fluids at  $T < ca. 300\text{ }^\circ\text{C}$  and  $P = ca. 0.7\text{ GPa}$  ( $M_2$ ). The extreme low- $T$  conditions during retrogression may have prevented reaction between eclogitic jadeite and adjacent minerals. Instead, eclogitic impure jadeite (plus fluid) has recrystallized into the retrograde jadeite + omphacite pair with a wide compositional gap.

### INTRODUCTION

Jadeitic pyroxene is ubiquitous in a variety of high-pressure (HP) and ultrahigh-pressure (UHP) metamorphic rocks; its parageneses and compositions often have been used to characterize HP-UHP rocks. Blueschist- and eclogite-facies clinopyroxenes are composed mainly of jadeitic and augitic components with minor amounts of an aegirine component (e.g., Maruyama and Liou 1987). Miscibility regions between jadeitic pyroxene ( $C2/c$ )–omphacite ( $P2/n$ ) and augitic pyroxene ( $C2/c$ )–omphacite ( $P2/n$ ) have been recognized along the augite [ $Ca(Mg,Fe)Si_2O_6$ ]–jadeite ( $NaAlSi_2O_6$ ) join (Carpenter 1980). Coexisting pairs of augitic pyroxene + omphacite have been reported from some blueschist-facies rocks (e.g., Enami and Tokonami 1984; Tsujimori 1997; Tsujimori and Liou 2004). On the other hand, coexisting jadeitic pyroxene and omphacite pairs in natural parageneses are rare except in jadeitites (e.g., Harlow 1994); hence the nature and extent of the jadeitic pyroxene–omphacite miscibility gap remains uncertain. Because there are no experimental studies to constrain the miscibility gap at low- $T$  ( $<400\text{ }^\circ\text{C}$ ), the occurrence of pyroxene pairs in nature is the only way to deduce the shape of the miscibility gap and to evaluate the theoretically proposed phase diagram.

As this paper newly reports, coexisting pairs of jadeitic pyroxene and omphacite occur as inferred retrograde products of impure jadeite in a sample of jadeite-bearing, lawsonite-eclogite

from the Motagua Fault Zone in Guatemala. The eclogite from this locality contains impure jadeite instead of omphacite, in addition to garnet, rutile, lawsonite, and quartz as inferred peak-stage minerals. During retrogression (accompanied by deformation), the impure jadeite partly recrystallized to a jadeite + (minor) omphacite pair corresponding to the possible miscibility gap. In this paper, we describe the parageneses and compositions of sodic pyroxenes formed during prograde and retrograde recrystallization. Mineral abbreviations are after Kretz (1983) excepting aegirine (Ae), ferroglaucophane (Fgl), and phengite (Phe) throughout this paper.

### GEOLOGIC SETTING

The Motagua Fault Zone (MFZ) is part of the suture zone juxtaposing the Maya and Chortís continental blocks in Guatemala. The left-lateral, strike-slip faults of the MFZ separate the present-day North American plate from the Caribbean plate. An eastern extension of the MFZ crosses the Caribbean Sea and lies along the Swan Islands fracture zone. Along the MFZ of central Guatemala, serpentinite bodies are exposed on either side of the Río Motagua (e.g., Beccaluva et al. 1995; Harlow et al. 2003, 2004) (Fig. 1). Some of the serpentinites are well known as world-class localities of jadeitite (e.g., Harlow 1994), and some also contain meter-size blocks of medium- $P$  and high- $P$  (HP) metamorphic rocks such as amphibolite, blueschist, and eclogite (McBirney et al. 1967; Harlow et al. 2003). The jadeitite and other HP rocks to the north of the MFZ yield phengite

\* E-mail: tatsukix@pangea.stanford.edu

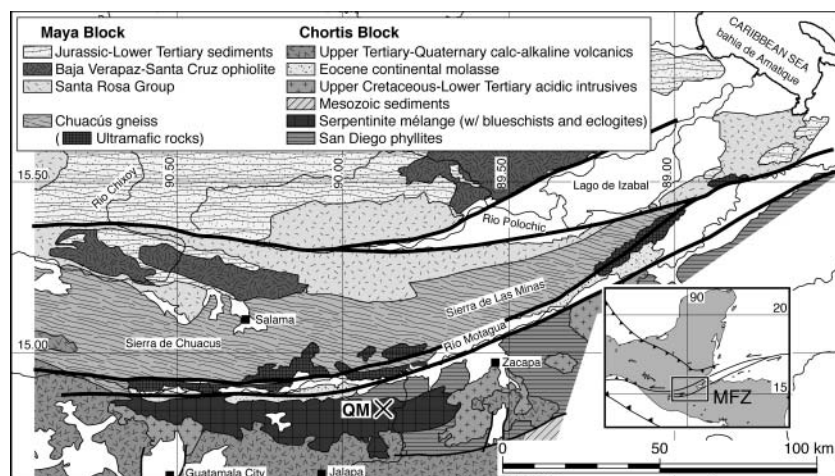


FIGURE 1. Simplified geologic map of the Motagua Fault Zone, Guatemala (modified from Beccaluva et al. 1995 and Martens et al. 2005), showing sampling locality at the Quebrada del Mico (QM).

$^{39}\text{Ar}$ - $^{40}\text{Ar}$  integrated ages of 65–77 Ma, whereas the jadeitites and eclogite/blueschist to the south of the MFZ have phengite  $^{39}\text{Ar}$ - $^{40}\text{Ar}$  integrated ages of 116–125 Ma (Harlow et al. 2004). A southern eclogite gives a Nd-Sm garnet–omphacite–whole-rock isochron age of 135 Ma (Sisson et al. 2003).

The investigated jadeite-bearing lawsonite-eclogite (JLEC) was collected as a loose block (6 × 8 m) in landslide debris of a 0.5 × 4 km fault-bounded eclogitic mélangé unit in a serpentinite mélangé along the Quebrada del Mico, a tributary of Río Jalapa and Río El Tambor, located south of the MFZ. The JLEC occurs as tectonic blocks surrounded by antigorite, and it is associated with fine- to medium-grained lawsonite-eclogites (sodic pyroxenes are commonly omphacitic), garnet-bearing lawsonite-blueschist, quartz-phengite schist, omphacitite, and jadeite (Tsuji-mori et al. 2003).

### PETROGRAPHY

The JLEC is weakly foliated, and characterized by the occurrence of unusually large garnet porphyroblasts up to 1.5–2.5 cm in diameter (Figs. 2a and 2b). The investigated sample consists mainly of sodic pyroxenes (~60 vol%) and garnet (~30 vol%), with minor amounts of rutile, phengite, chlorite, ferroglauco-phane, lawsonite, titanite, ilmenite, and quartz. Garnet porphyroblasts contain mineral inclusions of sodic pyroxenes, rutile, ferroglauco-phane, quartz, lawsonite, and phengite; chlorite and ilmenite inclusions are restricted to the core of garnet. Preferred orientation of mineral inclusions in garnet defines an internal foliation (S1, Figs. 2a and 2c). Relatively large, elongated polycrystalline inclusions (up to 3 mm length) of sodic pyroxene are aligned parallel to the S1 fabric. In a few cases, discrete sodic pyroxene inclusions (<0.2 mm) are replaced by albite along grain boundaries. Composite mineral inclusions of sodic pyroxene + phengite and sodic pyroxene + ferroglauco-phane are rarely recognized at the rim. The weakly foliated matrix is composed mainly of sodic pyroxenes with minor amounts of lawsonite, rutile, quartz, and phengite; preferred orientation of phengite and fine-grained sodic pyroxenes define a foliation (S2) at a high angle to the internal fabric (S1) in garnet (Fig. 2a).

Two generations of jadeitic pyroxene are recognized according to their textures in the matrix: (1) eclogitic impure jadeite

(Jd-I) and (2) retrograde jadeite (Jd-II), which coexists with minor omphacite (Omp; Fig. 2). The impure jadeite (Jd-I) of the first generation occurs as coarse-grained subhedral tabular crystals (up to 1.5 mm in length) that locally exhibit undulatory extinction (Figs. 2d and 2e); fine oscillatory growth bands (<3 μm) parallel to growth faces are rarely developed in internal texture (Fig. 2f). The Jd-I is typically deformed and fragmented; its internal growth bands are slightly bent (Figs. 2g and 2h). In contrast, the jadeitic pyroxene of the second generation (Jd-II) occurs in fine-grained aggregates associated with minor amounts of omphacite (Figs. 2d, 2e, 2g, and 2h); Jd-II replace coarser-grained Jd-I pyroxene grains, indicating that the Jd-I underwent grain-size reduction by recrystallization during deformation. The Jd-II, along with minor omphacite, also fills open cavities of the Jd-I. This texture suggests fluid infiltration to crystallize new pyroxenes. In a few cases, Jd-II pyroxene grains are intergrown with omphacite (0.1–0.5 mm) in the matrix (Fig. 2i); omphacite and Jd-II crosscut each other. These spatial relations and textural intergrowths suggest their coeval crystallization from infiltrated fluids. Tsujimori (1997) described a similar textural intergrowth of diopside and omphacite filling microveins of omphacitite from SW Japan.

### MINERAL COMPOSITIONS

Electron microprobe analysis was carried out with a JEOL JXA-8900R at the Okayama University of Science. Quantitative analyses of rock-forming minerals were performed with 15 kV accelerating voltage, 12 nA beam current, and 3–5 μm beam size. Natural and synthetic silicates and oxides were used as standards for calibration. The CITZAF method was employed for matrix corrections. Representative analyses of various sodic pyroxenes and the other minerals in a sample of JLEC are listed in Table 1.

### Clinopyroxenes

The  $\text{Fe}^{2+}/\text{Fe}^{3+}$  ratios and end-member components for sodic pyroxene were calculated using an algorithm suggested by Harlow (1999). The analyzed clinopyroxene grains are nearly free of Ca-Tschermak component; their analyses are plotted in the Jd–Aug (Di + Hd)–Ae ternary diagram of Figure 3.

Eighty-five points were analyzed on twelve impure jadeite (Jd-I) grains; each grain is rather homogeneous. They contain a nearly constant augite component of 16.1–23.6 mol%; major

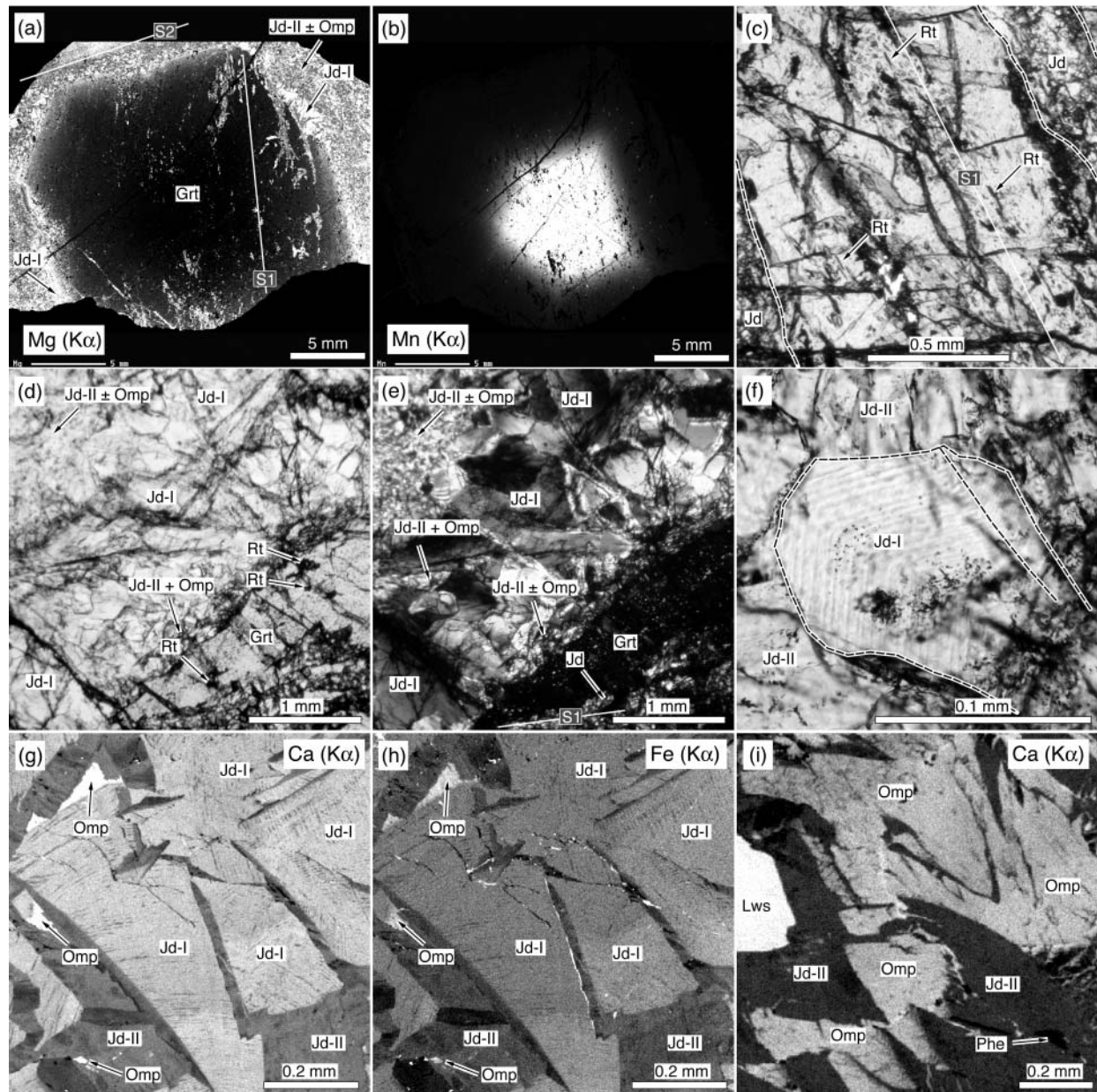


**FIGURE 2.** Microtextures of the investigated lawsonite-eclogite. (a) X-ray image of  $MgK\alpha$  of a garnet porphyroblast. Mg content of garnet (Grt) increases from core to rim. Garnet has an internal fabric (S1) at high angle to the matrix foliation S2. (b) X-ray image of  $MnK\alpha$  of a. Mn content decreases rimward, showing the form of near-euhedral polygons. (c) Enlarged photomicrograph showing internal fabric in a garnet porphyroblast [Plane polarized light = PPL]. Acicular rutile grains are aligned with a penetrative S1 fabric. (d) Photomicrograph of two generations of sodic pyroxenes adjacent to garnet [PPL]. See text for details. (e) Cross-polarized light view of d. (f) Enlarged photomicrograph of primary impure jadeite (Jd-I) [PPL]. Broken lines indicate optical grain boundaries. (g) X-ray image of  $CaK\alpha$  of retrograde jadeite (Jd-II) and omphacite (Omp) filling open cavities of impure jadeite (Jd-I). (h) X-ray image of  $FeK\alpha$  of g. (i) X-ray image of  $CaK\alpha$  of intergrowth of retrograde jadeite (Jd-II) and omphacite (Omp).

variations are along the Jd–aegirine join with Jd ranging from 61.2 to 75.0%, and Ae from 0 to 17.8%. All analyses plot near the boundary between the omphacite and jadeite fields of Morimoto et al. (1988; Fig. 3a). The  $X_{Mg}$  [=  $Mg/(Mg + Fe^{2+})$  atomic ratio] ranges from 0.44 to 0.93. Some coarser grains show chemical zoning; the core contains up to 7.4 wt% FeO whereas the rim

contains 5.0–5.5 wt% FeO.

Analyses of retrograde jadeite (Jd-II, 103 points on multiple grains) have much more restricted compositions compared to those of Jd-I (Fig. 3a). They are characterized by a significantly higher Jd component (Fig. 3a) of 74.4–86.5%, Aug = 8.5–16.1%, and Ae = 0–10.8%. The  $X_{Mg}$  varies from 0.30 to 0.90. Ompha-

**TABLE 1.** Representative analyses of various sodic pyroxenes and the other minerals

ID no.	Eclogitic Cpx (Jd-I)				Retrograde Cpx				Inclusions in Garnet					Garnet				
	core		rim		Jd-li	Jd-li	Omp	Omp	Cpx 2	Cpx 3	Cpx	Cpx	Phe	Fgl	Lws	rim 1	rim 2	core 3
SiO <sub>2</sub>	57.58	57.38	56.89	57.28	58.24	57.81	55.99	55.80	57.21	57.63	58.71	55.46	53.32	56.23	38.91	37.84	36.90	37.25
TiO <sub>2</sub>	0.06	0.06	0.08	0.11	0.09	0.05	0.04	0.06	0.03	0.02	0.05	0.13	0.17	0.03	0.15	0.07	0.17	0.31
Al <sub>2</sub> O <sub>3</sub>	17.43	16.98	16.16	16.65	20.26	19.89	10.74	10.89	16.75	17.30	21.71	12.17	24.13	11.45	31.38	21.12	21.29	20.28
Cr <sub>2</sub> O <sub>3</sub>	0.00	0.00	0.16	0.01	0.00	0.00	0.04	0.00	0.00	0.00	0.00	0.00	0.00	0.00	0.13	0.00	0.00	0.00
FeO*	5.61	5.41	7.49	5.54	3.69	4.16	6.46	7.62	6.01	5.17	2.90	8.75	3.07	17.13	0.52	31.56	32.77	27.46
MnO	0.09	0.03	0.04	0.09	0.06	0.04	0.00	0.02	0.13	0.10	0.03	0.09	0.03	0.06	0.00	0.08	0.08	6.68
MgO	2.33	2.76	2.68	2.85	1.47	1.50	6.83	6.11	2.76	2.88	0.97	4.28	4.53	5.30	0.00	2.06	1.59	0.34
CaO	5.13	5.59	5.40	5.59	2.85	3.09	11.74	11.34	5.93	5.26	2.16	10.30	0.03	0.33	17.10	8.09	7.69	8.56
Na <sub>2</sub> O	11.98	11.65	11.33	11.72	13.07	13.08	8.03	8.17	11.68	11.45	13.45	8.97	0.16	7.41	0.01	0.06	0.04	0.00
K <sub>2</sub> O	0.00	0.03	0.00	0.03	0.00	0.00	0.00	0.00	0.03	0.01	0.01	0.01	8.93	0.00	0.01	0.00	0.00	0.00
Total	100.20	99.88	100.23	99.87	99.73	99.63	99.87	100.01	100.53	99.82	99.99	100.16	94.37	97.93	0.00	100.89	100.52	100.89
O=	6	6	6	6	6	6	6	6	6	6	6	6	11	23	8	12	12	12
Si	2.001	2.001	1.993	1.997	2.010	1.998	1.992	1.990	1.985	2.012	2.011	1.979	3.559	7.944	2.039	2.999	2.956	2.997
Ti	0.001	0.001	0.002	0.003	0.002	0.001	0.001	0.002	0.001	0.001	0.001	0.004	0.009	0.003	0.006	0.004	0.010	0.019
Al	0.714	0.698	0.667	0.684	0.824	0.810	0.450	0.458	0.685	0.712	0.877	0.512	1.898	1.906	1.938	1.973	2.010	1.923
Cr	0.000	0.000	0.004	0.000	0.000	0.000	0.001	0.000	0.000	0.000	0.000	0.000	0.000	0.000	0.005	0.000	0.000	0.000
Fe <sup>3+</sup>	0.089	0.086	0.107	0.108	0.026	0.067	0.117	0.124	0.130	0.039	0.000	0.145	0.071	0.023				
Fe <sup>2+</sup>	0.074	0.071	0.112	0.053	0.080	0.053	0.075	0.103	0.045	0.112	0.083	0.117	0.171	1.953	2.092	2.195	1.848	
Mn	0.003	0.001	0.001	0.003	0.002	0.001	0.000	0.001	0.004	0.003	0.001	0.003	0.002	0.007	0.005	0.006	0.455	
Mg	0.121	0.143	0.140	0.148	0.076	0.077	0.362	0.325	0.143	0.150	0.050	0.228	0.451	1.116	0.000	0.243	0.189	0.041
Ca	0.191	0.209	0.203	0.209	0.105	0.114	0.447	0.433	0.221	0.197	0.079	0.394	0.002	0.050	0.960	0.687	0.660	0.738
Na	0.807	0.788	0.770	0.792	0.875	0.877	0.554	0.565	0.786	0.775	0.893	0.621	0.021	2.030	0.001	0.009	0.006	0.000
K	0.000	0.001	0.000	0.001	0.000	0.000	0.000	0.000	0.001	0.000	0.000	0.000	0.760	0.000	0.000	0.001	0.000	0.000
X <sub>Mg</sub>	0.62	0.67	0.56	0.74	0.49	0.59	0.83	0.76	0.76	0.57	0.37	0.66	0.72	0.36	0.10	0.08	0.02	

Notes: FeO\* = total Fe as FeO. X<sub>Mg</sub> = Mg/(Mg + Fe<sup>2+</sup>). The ID no. represents the analyzed minerals that are adjacent to each other.

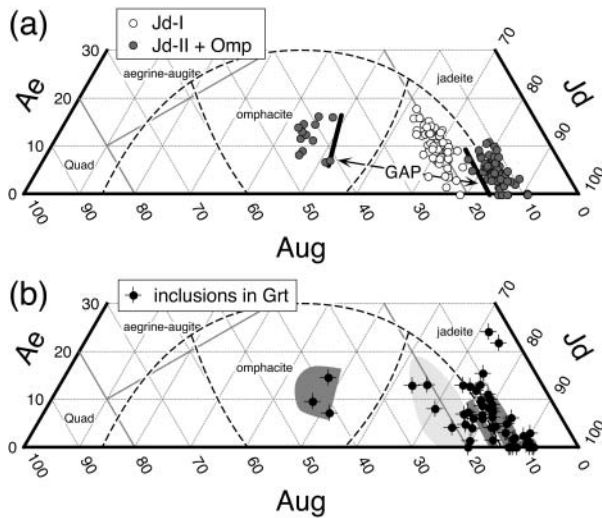


**FIGURE 3.** Compositions of analyzed clinopyroxenes from two metamorphic stages on the Jd–Aug–Ae ternary diagram. Phase relations in the Jd–Aug–Ae system proposed by Carpenter (1980) are also shown as dashed lines. (a) Eclogitic impure jadeite (Jd-I) and retrograde jadeite (Jd-II) + omphacite (Omp). The apparent compositional gap is shown as bold lines. (b) Sodic pyroxene inclusions in a garnet porphyroblast. Gray areas show the compositional field of the Jd-I, Jd-II and Omp plotted in a.

cite grains coexisting with retrograde jadeite (12 analyses on multiple grain, have compositions of Jd = 41.5–50.2%, Aug = 35.9–46.0%, and Ae = 6.7–16.4%, with X<sub>Mg</sub> = 0.70–0.88. No systematic chemical zoning was observed in either retrograde jadeite or omphacite.

Sodic pyroxene inclusions in a garnet porphyroblast (53 analyses on multiple grains) show a wide compositional variation; the analyses mostly overlap the compositional ranges of the

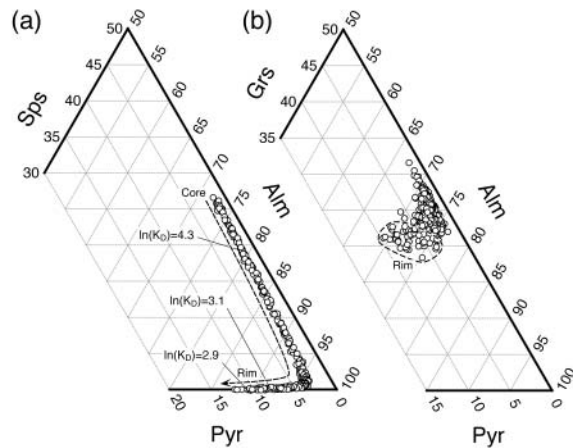


**FIGURE 4.** Compositions of analyzed garnets on (a) the Pyr–Alm–Sps and (b) Pyr–Alm–Grs ternary diagrams. The dashed arrow in b represents the compositional trend of garnets from core to rim; the representative values of the Fe<sup>2+</sup>-Mg partitioning ( $K_D$ ) between eclogitic impure jadeite and adjacent garnet are also shown.

Jd-I, Jd-II, and Omp described above (Fig. 3b). Jadeitic pyroxene grains with compositions similar to Jd-I are interpreted as Jd-I that survived recrystallization.

**Garnet**

Garnet porphyroblasts are rich in the almandine (Alm) component with moderate grossular (Grs) and low pyrope (Pyr) and spessartine (Sps) (Alm<sub>54.8-76.0</sub>Grs<sub>17.4-28.3</sub>Pyr<sub>0.9-9.7</sub>Sp<sub>0.21.8</sub>); the X<sub>Mg</sub> ranges from 0.02 to 0.12. Garnet porphyroblasts show distinct, prograde, bell-shaped chemical zoning of Mn (Fig. 2b); the pyrope content increases from core to rim (Fig. 4a), and the grossular content slightly decreases at the outer rim (Fig. 4b).

This feature implies a progressive increase in temperature during the growth of the garnet porphyroblasts (e.g., Sakai et al. 1985; Enami 1998). In fact, the Fe<sup>2+</sup>-Mg partitioning ( $K_D$ ) between primary sodic pyroxene inclusions and the adjacent garnet host is smaller at the rim than the core (Fig. 4a).

### Other minerals

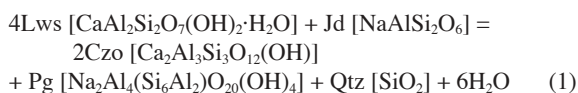
Ferroglaucofane inclusions in garnet are low in Ca (<0.7 wt% CaO), and the  $X_{Mg}$  ranges from 0.18 to 0.46. The inferred Fe<sup>3+</sup>/(Fe<sup>3+</sup> + Al) ratio is less than 0.2. Phengite inclusions in garnet have 3.5–3.6 Si p.f.u. (O = 11) and the  $X_{Mg}$  values range from 0.69 to 0.73. Lawsonite inclusions in garnet and matrix contain less than 0.2 wt% Fe<sub>2</sub>O<sub>3</sub>.

### P-T CONDITIONS OF METAMORPHISM

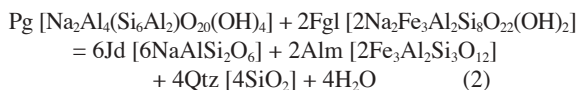
Textural relations, mineral parageneses, and mineral compositions indicate that the investigated lawsonite-eclogite experienced at least two stages of metamorphic recrystallization: a *P-T* evolution from a prograde eclogite-facies stage (M<sub>1</sub>) to retrograde stage (M<sub>2</sub>) was identified.

### Eclogite-facies stage (M<sub>1</sub>)

The prograde eclogite-facies stage produced the assemblage Grt + Jd-I (Jd<sub>75</sub>) + Lws + Phe + Fgl + Rt + Qtz. The Jd + Qtz + Ab sliding equilibrium (Holland 1983), and Grt-Cpx thermometry (Ravna 2000) of the Jd inclusion with primary composition + adjacent Grt core, and of matrix Jd-I + adjacent Grt rim give a minimum  $P = 0.8$ –1.0 GPa at  $T = ca. 300$ –420 °C for the eclogite-facies stage (Fig. 5). This *P-T* condition is consistent with the occurrence of the Jd + Lws assemblage instead of Czo + Pg, as defined by the following reaction:



Moreover, the equilibrium proposed by Miyazaki et al. (1998)



further constrains the minimum  $P > 1.6$ –2.0 GPa at  $T = ca. 340$ –430 °C for the Grt + Jd + Qtz ± Fgl assemblage (Fig. 5). Because neither coesite nor evidence of quartz pseudomorphs after coesite were found, the eclogite-facies stage is restricted within the quartz stability field of  $P < 2.4$ –2.5 GPa at  $T = ca. 360$ –470 °C. However, Grt-Cpx-Phe barometry (Carswell et al. 1997) of composite mineral inclusions at the rim of Grt yield very high-pressure conditions ( $P = ca. 2.7$  at  $T = ca. 450$  °C; Fig. 5). The peak *P-T* condition of the eclogite-stage lies very close to the coesite stability field. The experimentally proposed petrogenetic grid of the lawsonite-eclogite facies (Okamoto and Maruyama 1999) and the occurrence of coesite in lawsonite-eclogite xenoliths from the Colorado Plateau (Usui et al. 2003) support our estimated  $P$  near UHP conditions. Further study of mineral inclusions in zircon separates from eclogites and metapelites is necessary to confirm such a suggestion.

### Retrograde stage (M<sub>2</sub>)

As described above, some pyroxene textures suggest the introduction of fluid to crystallize M<sub>2</sub> minerals. Fluid infiltration also may have promoted subsolidus recrystallization. In any case, the mineral assemblage constrains the *P-T* conditions. The retrograde stage is characterized by the presence of coexisting sodic pyroxenes with a wide compositional gap, rare albite, and quartz and titanite instead of rutile. Both lawsonite and garnet apparently remained stable. This assemblage is similar to commonly reported blueschist-facies assemblages (e.g., Maruyama et al. 1996). Using the composition of Jd-II and the Jd + Qtz + Ab sliding equilibrium (Holland 1983), we obtain approximate *P-T* conditions of  $P = ca. 0.7$  GPa and  $T < ca. 300$  °C. This result implies that the retrograde jadeite and omphacite may have formed at blueschist-facies condition.

### MISCIBILITY GAP BETWEEN JADEITIC PYROXENE AND OMPHACITE

In the Jd-Aug system, the ordering of cations on the M1 and M2 sites occurs in intermediate compositions (omphacite),

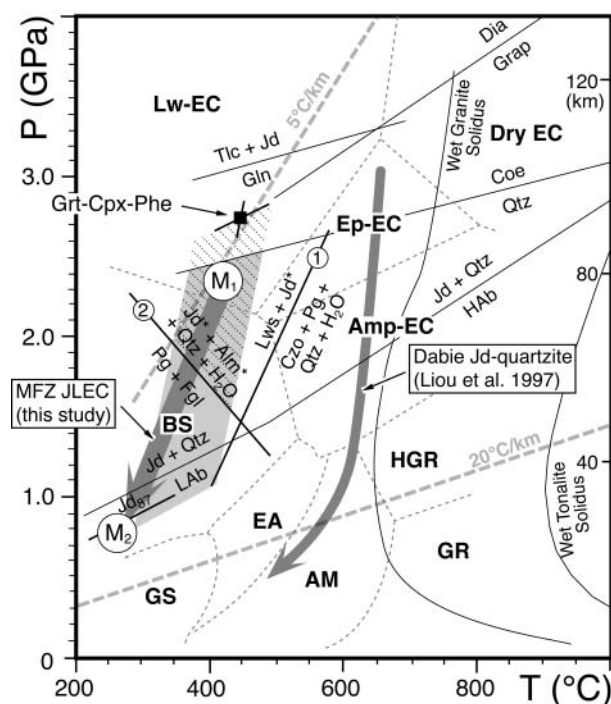
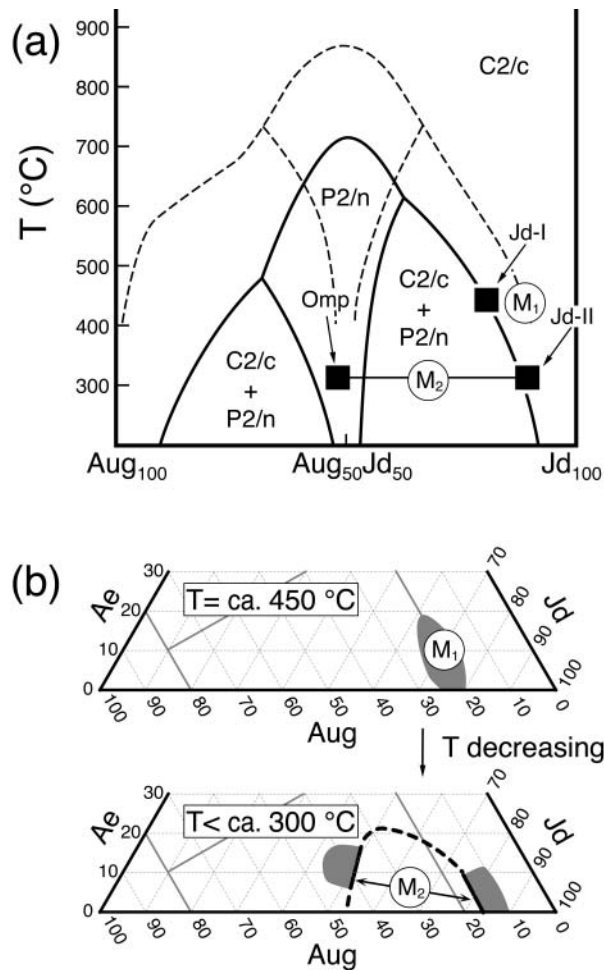


FIGURE 5. *P-T* diagram showing a qualitative retrograde *P-T* path, from the M<sub>1</sub> to M<sub>2</sub>, of the investigated lawsonite-eclogite. Hatched area represents the estimated conditions of the prograde eclogite-facies stage (M<sub>1</sub>) and retrograde stage (M<sub>2</sub>); grayed area represents a *P-T* field constrained by the Jd + Qtz sliding equilibrium (Holland 1983), and Grt-Cpx thermometry (Ravna 2000). The reactions (1) and (2) were calculated using THERMOCALC (ver. 3.21) program (Powell et al. 1998); activity models for ferroglaucofane and almandine followed Miyazaki et al. (1998). Filled square represents a *P-T* estimation using the Grt-Cpx-Phe thermobarometer (Carswell et al. 1997). The metamorphic facies, their abbreviations, and other information are from Liou et al. (2004). Retrograde *P-T* path of the jadeite-quartzite from the Sulu UHP terrane (Liou et al. 1997) is shown for comparison.



**FIGURE 6.** (a)  $T$ - $X$  (Jd component in Jd-Aug solid-solution) phase diagram of the Jd-Aug binary system. Solid lines represent phase relations proposed by Carpenter (1980). Broken lines indicate phase relations proposed by Vinograd (2002). The compositions of the investigated pyroxenes are also shown as filled squares. (b) The compositional trend of sodic pyroxenes of the investigated eclogite (grayed areas) showing a possible miscibility gap (bold lines) in the Jd-Aug-Ae system.

causing a symmetry change from  $C$ -face-centered to primitive. As a result, continuous substitution does not occur in the system at low-temperature. A miscibility gap between jadeite and omphacite was first suggested by Coleman and Clarke (1968) based on studies of California blueschists. Numerous theoretical and experimental studies propose different mixing properties for Jd-Aug solid solutions; some studies delineated the phase relations as function of  $P$  and  $T$  (e.g., Carpenter 1980, 1990; Holland 1983, 1990; Nakamura and Banno 1997; Vinograd 2002). For example, Carpenter (1980) proposed a  $T$ - $X$  (composition) diagram for ordered  $P2/n$  and disordered  $C2/c$  pyroxenes, as shown by the solid lines of Figure 6A; his model is based on a second-order transformation mechanism. The apparent critical temperature for the solvus between  $C2/c$  jadeite and  $P2/n$  omphacite is about 600 °C. Recently Vinograd (2002) theoretically

reproduced the shape of the phase diagram proposed by Carpenter (1980), but with much higher critical temperatures, as shown by the dashed lines of Figure 6a. Although the asymmetry and critical  $T$  of two solvi are different in the two studies, the solvus between  $C2/c$  jadeite and  $P2/n$  omphacite becomes wider with decreasing temperature in both of them (Fig. 6a).

The observed parageneses and compositions of Jd-I at higher  $T$  and paired jadeite and omphacite compositions at lower  $T$  described above are consistent with the phase diagram of Carpenter (1980), although we cannot constrain the upper limb of the solvus. Based on his phase diagram, the following scenario is proposed for the investigated sample (Figs. 6a and 6b). First, the jadeitic pyroxene of the  $M_1$  eclogite-facies stage ( $T \sim 450$  °C) formed, with a maximum Jd content of 75% and a disordered  $C2/c$  symmetry. During exhumation of the eclogitic slab, the eclogite suffered  $M_2$  retrogression at blueschist-facies conditions ( $T < 300$  °C); both retrograde jadeite with higher Jd (maximum Jd = 87%) and the ordered  $P2/n$  omphacite (Jd = 42–50%) were recrystallized from the impure jadeite, and/or from infiltrated fluid during deformation. Our data also suggest that the miscibility gap between jadeite and omphacite at  $T < \text{ca. } 300$  °C may be asymmetrical in shape within the Jd-Aug-Ae system; the gap becomes narrower with increasing Ae content (Fig. 6b).

Impure jadeitic pyroxenes have been reported in some UHP eclogite-facies metamorphosed quartzites and granitic rocks at moderate- $T$  (e.g., Zhang et al. 1995; Gil Ibarra 1995; Liou et al. 1997). However, these jadeitic pyroxenes did not recrystallize into jadeite + omphacite during retrogression. Jadeitic pyroxenes from UHP rocks commonly reacted with quartz to form amphibole + sodic plagioclase through hydration reactions with adjacent minerals under amphibolite-facies conditions. In the investigated sample, the retrograde  $P$ - $T$  trajectory lies at extremely low- $T$  conditions, under which jadeite-rich pyroxene is stable with quartz (Fig. 5). The extremely low- $T$  conditions during retrogression may have prevented reaction between eclogitic jadeite and adjacent minerals. Hence, impure jadeite in the eclogite recrystallized and transformed into the jadeite + omphacite pair with a wide compositional gap. At the same time, these pyroxene pairs also crystallized from fluids that may have promoted recrystallization of primary impure jadeite.

#### ACKNOWLEDGMENTS

We dedicate this paper to our dear friend and mentor, W. Gary Ernst, who was the first to propose similar prograde and retrograde  $P$ - $T$  paths for preservation of jadeite and aragonite in the Franciscan-type blueschist terranes. This research was supported financially in part by a JSPS Research Fellowship for Research Abroad to the first author. Preparation of this manuscript was supported by NSF EAR-0003355. We thank William Rohtert, John Cleary, and Pieter Lee of Ventana Mining Company for their help in the field work. This manuscript was greatly improved by constructive comments from George E. Harlow and Bernard W. Evans. We thank the above-named individuals and institutions for their support and help.

#### REFERENCES CITED

- Beccaluva, L., Bellia, S., Coltorti, M., Dengo, G., Giunta, G., Mendez, J., Romero, J., Rotolo, S., and Siena, F. (1995) The northwestern border of the Caribbean plate in Guatemala: New geological and petrological data on the Motagua ophiolitic belt. *Ophioliti*, 20, 1–15.
- Carpenter, M.A. (1980) Mechanisms of exsolution in sodic pyroxenes. *American Mineralogist*, 64, 102–108.
- (1990) Application of Landau theory to cation ordering in omphacite I: Equilibrium behavior. *European Journal of Mineralogy*, 2, 7–18.
- Carswell, D.A., O'Brien, P.J., Wilson, R.N., and Zhai, M. (1997) Thermobarometry of phengite-bearing eclogites in the Dabie Mountains of central China. *Journal*

- of Metamorphic Geology, 15, 239–252.
- Coleman, R.G. and Clark, J.R. (1968) Pyroxenes in the blueschist facies of California. *American Journal of Science*, 266, 43–59.
- Enami, M. (1998) Pressure-temperature path of Sanbagawa prograde metamorphism deduced from grossular zoning of garnet. *Journal of Metamorphic Geology*, 16, 97–106.
- Enami, M. and Tokonami, M. (1984) Coexisting sodic diopside and omphacite in a Sanbagawa metamorphic rock, Japan. *Contributions to Mineralogy and Petrology*, 86, 241–247.
- Harlow, G.E. (1994) Jadeitites, albitites and related rocks from the Montagua Fault Zone, Guatemala. *Journal of Metamorphic Geology*, 12, 49–68.
- — — (1999) Interpretation of Kcpx and CaEs components in clinopyroxene from diamond inclusions and mantle samples. In J.J. Gurney, J.L. Gurney, M.D. Pascoe, and S.H. Richardson, Eds., *Proceedings of Seventh International Kimberlite Convention*, Vol. I, 321–331, Redroof Design Cc, Cape Town.
- Harlow, G.E., Sisson, V.B., Avé Lallemand, H.G., Sorensen, S.S., and Seitz, R. (2003) High pressure metasomatic rocks along the Motagua Fault Zone, Guatemala. *Ophiolite*, 28, 115–120.
- Harlow, G.E., Hemming, S.R., Sisson, V.B., and Sorensen, S.S. (2004) Two high-pressure–low-temperature serpentinite-matrix melange belts, Motagua fault zone, Guatemala: A record of Aptian and Masstrichtian collisions. *Geology*, 32, 17–20.
- Holland, T.J.B. (1983) The experimental determination of activities in disordered and short-range ordered jadeitic pyroxenes. *Contributions to Mineralogy and Petrology*, 82, 214–220.
- — — (1990) Activities of components in omphacitic solid solutions. *Contributions to Mineralogy and Petrology*, 105, 446–453.
- Kretz, R. (1983) Symbols for rock-forming minerals. *American Mineralogist*, 68, 277–279.
- Gil Ibarra, J.I. (1995) Petrology of jadeite metagranite and associated orthogneiss from the Malpica-Tuy allochthon (Northwest Spain). *European Journal of Mineralogy*, 7, 403–415.
- Liou, J.G., Zhang, R.Y., and Jahn, B.M. (1997) Petrogenesis of ultrahigh-pressure jadeite quartzite from the Dabie region, east-central China. *Lithos*, 41, 59–78.
- Liou, J.G., Tsujimori, T., Zhang, R.Y., Katayama, I., and Maruyama, S. (2004) Global UHP metamorphism and continental subduction/collision: The Himalayan model. *International Geology Review*, 46, 1–27.
- Maruyama, S., Liou, J.G., and Terabayashi, M. (1986) Blueschists and eclogites of the world, and their exhumation. *International Geology Review*, 38, 485–594.
- Martens, U., Ortega-Obregón, C., Valle, M., and Estrada-Carmona, J. (2005) Metamorphism and Metamorphic Rocks. In J. Bundschuh and G. Alvarado, Eds., *Central America: Geology, Resources, and Natural Hazards*. A.A. Balkema Publishers, Lisse, the Netherlands, in press.
- Maruyama, S. and Liou, J.G. (1987) Clinopyroxene—a mineral telescoped through the processes of blueschist facies metamorphism. *Journal of Metamorphic Geology*, 5, 529–552.
- McBirney, A., Aoki, K., and Bass, M.N. (1967) Eclogites and jadeite from the Motagua fault zone, Guatemala. *American Mineralogist*, 52, 908–918.
- Miyazaki, K., Sopaheluwakan, J., Zulkarnain, I., and Wakita, K. (1998) A jadeite-quartz-glaucophane rock from Karangsambung, central Java, Indonesia. *The Island Arc*, 7, 223–230.
- Morimoto, N., Fabries, J., Ferguson, A.K., Ginzburg, I.V., Ross, M., Seifert, F.A., Zussman, J., Aoki, K., and Gottardi, G. (1988) Nomenclature of pyroxenes. *American Mineralogist*, 73, 1123–1133.
- Nakamura, D. and Banno, S. (1997) Thermodynamic modeling of sodic pyroxene solid-solution and its application in a garnet-omphacite-kyanite-coesite geothermobarometer for UHP metamorphic rocks. *Contributions to Mineralogy and Petrology*, 130, 93–102.
- Okamoto, K. and Maruyama, S. (1999) The high-pressure synthesis of lawsonite in the MORB+H<sub>2</sub>O system. *American Mineralogist*, 84, 362–373.
- Powell, R., Holland, T.J.B., and Worley, B. (1998) Calculating phase diagrams involving solid solutions via non-linear equations with examples using THERMOCALC. *Journal of Metamorphic Geology*, 16, 577–588.
- Ravna, E.K. (2000) The garnet–clinopyroxene Fe<sup>2+</sup>–Mg geothermometer: an updated calibration. *Journal of Metamorphic Geology*, 18, 211–219.
- Sakai, C., Banno, S., Toriumi, M., and Higashino, T. (1985) Growth history of garnet in pelitic schists of the Sanbagawa metamorphic terrain in central Shikoku. *Lithos*, 18, 81–95.
- Sisson, V.B., Harlow, G.E., Sorensen, S.S., Brueckner, H.K., Sahn, E., Hemming, S., and Avé Lallemand, H.G. (2003) Lawsonite eclogite and other high-pressure assemblages in the southern Motagua Fault zone, Guatemala: Implications for Chortís collision and subduction zones. *Geological Society of America Abstracts with Programs*, 35, 639.
- Tsujimori, T. (1997) Omphacite-diopside vein in an omphacite block from the Osayama serpentinite melange, Sangun-Renge metamorphic belt, southwestern Japan. *Mineralogical Magazine*, 61, 845–852.
- Tsujimori, T. and Liou, J.G. (2004) Coexisting chromian omphacite and diopside in tremolite schist from the Chugoku Mountains, SW Japan: The effect of Cr on the omphacite-diopside immiscibility gap. *American Mineralogist*, 89, 7–14.
- Tsujimori, T., Liou, J.G., Coleman, R.G., and Rohtert, W. (2003) Eclogitization of a cold subducting slab: Prograde evolution of lawsonite-eclogites from the Motagua Fault Zone, Guatemala. *Geological Society of America Abstracts with Programs*, 35, 639.
- Usui, T., Nakamura, E., Kobayashi, K., and Maruyama, S. (2003) Fate of the subducted Farallon Plate inferred from eclogite xenoliths in the Colorado Plateau. *Geology*, 31, 589–592.
- Vinograd, V.L. (2002) Thermodynamics of mixing and ordering in the diopside-jadeite system: I. A CVM model. *Mineralogical Magazine*, 66, 513–536.
- Zhang, R.Y., Hirajima, T., Banno, S., Cong, B., and Liou, J.G. (1995) Petrology of ultrahigh-pressure rocks from the southern Sulu region, eastern China. *Journal of Metamorphic Geology*, 13, 659–675.

MANUSCRIPT RECEIVED MAY 6, 2004

MANUSCRIPT ACCEPTED JANUARY 28, 2005

MANUSCRIPT HANDLED BY SORENA SORENSEN